Vol. 37, No. 2 (2015) 244-256

Tribology in Industry

www.tribology.fink.rs.fink.rs

RESEARCH

Wear and Friction Behavior of in-situ AA5052/ZrB_2Composites under Dry Sliding Conditions

N. Kumar[a], R.K. Gautam[b], S. Mohan[c]

[a]*Bundelkhand Institute of Engineering and Technology, Department of Mechanical Engineering, Jhansi, India,*
[b]*Indian Institute of Technology, Department of Mechanical Engineering, Varanasi, India,*
[c]*Centre of Advanced Study, Indian Institute of Technology, Department of Metallurgical Engineering, Varanasi, India.*

Keywords:

In-situ composites
ZrB_2 particles
Wear
Friction
Mild-oxidative
Severe-metallic

Corresponding author:

N. Kumar
Bundelkhand Institute of Engineering and Technology,
Department of Mechanical Engineering, Jhansi, India.
E-mail: narendra.dharwan@gmail.com

A B S T R A C T

In-situ AA5052/ZrB_2 composites with different volume percentage (0,3, 6 and 9 vol.%) of zirconium diboride (ZrB_2) particles were successfully prepared by in-situ reaction between two inorganic salts potassium-hexa-fluoro-zirconate (K_2ZrF_6), potassium tetra-fluoro-borate (KBF_4) and aluminum alloy AA5052 at 860 °C. The composites were characterized by X-ray diffractometer (XRD) for the confirmation of in-situ formed ZrB_2 particles. Optical microscopy examination reveals the grain refinement of Al-rich grains due to in-situ formed ZrB_2 particles. Scanning electron microscope (SEM) and Energy dispersive X-ray spectroscopy (EDS) studies were carried out to reveal the morphology, distribution and secondary confirmation of ZrB_2 particles in the matrix. Transmission electron microscope (TEM) analysis was done to reveal the crystal structure, interfacial characteristics and dislocations around the ZrB_2 particles. Hardness of composites improved significantly as compared to base alloy. Dry sliding wear and friction study of composites was carried out at room temperature on pin-on-disc apparatus. The results revealed that cumulative weight loss of both the base alloy and composites shows a linear relationship with sliding distance, however, change in slope is observed at certain intervals. Wear rate decrease with formation of in-situ ZrB_2 particles and improves as the reinforcement amount increases, whereas, coefficient of friction of composites follows a reverse trend. Worn surfaces of pin samples reveal mild-oxidative and severe-metallic wear under scanning electron microscope.

1. INTRODUCTION

Aluminum matrix composites (AMCs) have been developed to meet the increasing demand of light weight, fuel efficient and high performance materials for automobile, aerospace, transportation and chemical industries. Either ex-situ or in-situ process may be employed for preparing the AMCs. However, the in-situ process is preferred over ex-situ, as it can overcome the problems of non-uniform distribution of reinforcement particles, poor bonding with the matrix interface, thermodynamic instability etc. [1-4]. Being very cost effective and having improved strength, high elastic modulus, high temperature properties and wear resistance etc., these AMCs are replacing their conventional alloys in manufacturing of various components like pistons, brake drums, engine block, cylinder liners, connecting rods, crankshafts [5-8]. Improved wear resistance makes AMCs potential candidate for tribological applications.

Various intermetallic and ceramics in the form of tri-aluminides, oxides, carbides, nitrides, borides or combination of these have been used by many workers to improve the tribological properties of AMCs [9-15]. Among various reinforcements ZrB_2 is considered to be more potentially viable due to its high stiffness, hardness, high melting point, high thermal and electrical conductivity, better wear resistance, good high temperature strength and most importantly it does not react with aluminum [16,17].

Zhang et al. [18,19] prepared A356 based composites reinforced with Al_3Zr and ZrB_2 particles by magneto chemistry in-situ reaction in Al-K_2ZrF_6-KBF_4 system and studied the microstructural and dry sliding wear properties. They observed regular hexagonal and tetragonal morphology of Al_3Zr and ZrB_2 particles with a size range of about 0.3-0.5 μm.

They also found that the weight loss of composites decreases with increased amount of K_2ZrF_6-KBF_4 powders. Kumar et al. [20] studied the dry sliding wear behavior of AA6351-ZrB_2 in-situ composites at room temperature in as cast, solutionized and solutionized–aged conditions. They observed that wear resistance of composites increases with increased ZrB_2 content and it was highest in case of solutionized- aged composites. Dinaharan et al. [21] studied the dry sliding wear behavior of AA6061/ZrB_2 in-situ composites and developed the mathematical models to predict the effect of sliding distance, sliding velocity, mass fraction of ZrB_2 and applied load on wear rate of composites. Chen et al. [22] studied the microstructural and dry sliding wear properties ofA356/ZrB_2 composites synthesized via magneto chemistry in-situ reaction in Al-K_2ZrF_6-KBF_4 system. They reported the reduction in weight loss of composites and change in wear mechanism from adhesion to abrasion with increased ZrB_2 content.

In view of the above, non-heat treatable Al-Mg alloy has been chosen as base alloy. Al-Mg alloys are also important because their strength is maintained with frictional heating [23-25]. AA5052 is an aluminum–magnesium alloy with low density, medium static strength, good formability, weldability, and corrosion resistance. Magnesium present in the alloy increases the strength without decreasing the ductility. Magnesium also compensates the increased density of composites due to the addition of ceramic particles. In the present study an effort is made to study the dry sliding wear and friction behavior of AA5052 aluminum alloy reinforced with in-situ formed ZrB_2 particles.

2. EXPERIMENTAL DETAILS

AA5052/ZrB_2 composites were prepared by AA5052 aluminum alloy with chemical composition as shown in Table 1 and two inorganic salts K_2ZrF_6 (97 % purity) and KBF_4 (96 % purity).

Table 1. Chemical composition of AA5052 alloy.

Element	Al	Mg	Si	Fe	Cu	Mn	Cr	Zn
wt%	96.78	2.5	0.13	0.3	0.01	0.05	0.2	0.03

Required amount of K_2ZrF_6 and KBF_4 salts were preheated in an electric oven at 250 °C for 3 hours to remove the moisture. Then the K_2ZrF_6 and KBF_4 salts were cooled, screened and properly mixed in the mass ratio of 52:48 to prepare the composite. Simultaneously required amount of AA5052 alloy was placed into a graphite crucible and allowed to heat at a constant rate of 300 °C/h in a vertical muffle furnace. Once the temperature of molten alloy reached to 860 °C, pre-heated suitable amount of inorganic salts was added to the molten alloy and maintained at 860 °C for 30 minutes to complete the in-situ reaction as given in eqn. 1 to 3 [26] while stirring intermittently with a zirconia coated graphite stirrer to distribute the in-situ formed ZrB_2 particles uniformly throughout the matrix. Thus, the composites of different compositions were prepared by varying the quantity of salts.

$$K_2ZrF_6 + 13/3Al = Al_3Zr + 4/3AlF_3 + 2KF \quad (1)$$

$$2KBF_4 + 3Al = AlB_2 + 2AlF_3 + 2KF \quad (2)$$

$$Al_3Zr + AlB_2 = ZrB_2 + 4Al \quad (3)$$

XRD (Rigaku) study was carried out for identification of second phase ZrB_2 particles in composites using Cu Kα radiation of wavelength 1.541836Å with Ni filter. Surface morphology, phase identification and distribution of in-situ formed ZrB_2 particles were examined under SEM (FESEM Quanta 200FEG) equipped with EDS. TEM (TECNAI G[2] 20) was used to reveal the crystal structure and high dislocation density created by fine ZrB_2 particles. TEM foils were prepared by electrolyte containing 90 % ethanol and 10 % perchloric acid cooled to -35 °C and 60 volts, using a twin jet polisher (FISHIONE, Model 110). Hardness of the base alloy and composites was estimated by Brinell Hardness Testing Machine (Aktiebolaget Alpha) at 500 Kgf load for a dwell time of 30 seconds.

To estimate the actual amount of ZrB_2 particles in the composites, ZrB_2 particles were extracted from the composite by dissolving the known weight of composite sample in 10 % HCl solution for several days. The aluminum matrix was dissolved in acid solution and then it was filtered with an ash less filter paper. Residue of ZrB_2 particles was thoroughly washed, dried and weighed. The difference in weights of the extracted particles and composite sample taken for analysis was calculated to get the actual amount of ZrB_2 particles. Actual volume fractions in the composites were found be 2.85 %, 5.58 % and 8.10 %.

Dry sliding wear and friction studies were carried out on pin-on-disc wear and friction testing machine with data acquisition system (Magnum Engineers, Bangalore, India) as schematically shown in Fig. 1.

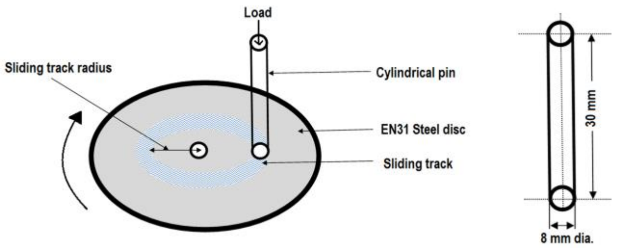

Fig. 1. Schematic diagram of pin-on-disc apparatus.

Cylindrical wear samples of 30 mm length and 8 mm diameter were used for wear and friction tests against a hardened steel disc of grade EN31. Wear tests were carried out at four different loads 10, 20, 30 and 40 N for a fixed sliding velocity of 2.12 m/s for a total sliding distance of about 6 Kilometres. All tests were conducted at room temperature under dry sliding conditions. After each test the pin sample was ultrasonically cleaned with acetone and weight loss was measured with a digital balance with least count of 0.1 mg. Wear rate was calculated from the weight loss measurements. Coefficient of friction was calculated from the frictional force and applied load values. Ratio of frictional force to applied load represents the value of coefficient of friction. Three samples were tested at each condition and average value is reported.

3. RESULTS AND DISCUSSION

3.1 XRD Analysis

Figure 2a shows the XRD pattern of in-situ developed AA5052/ZrB_2 composites with different composition 0, 3, 6, and 9 vol.% of ZrB_2 particles.

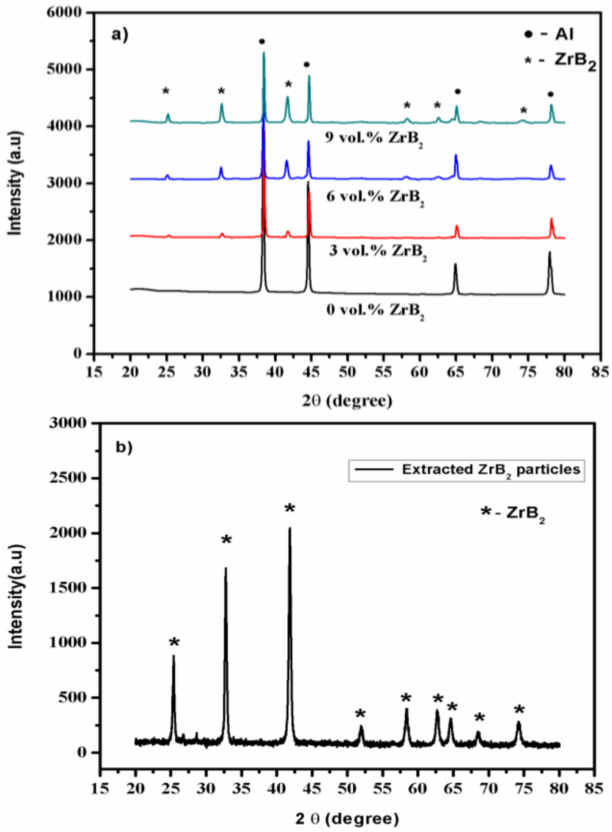

Fig. 2. XRD pattern of (a) Prepared in-situ composites (b) Extracted ZrB_2 particles.

Diffraction peaks of ZrB_2 particles were clearly seen for all compositions which confirm the presence of in-situ formed ZrB_2 particles. It was also observed that intensity of the ZrB_2 diffraction peaks increases with increasing the volume fraction of ZrB_2 particles. Peaks of other probable phases such as intermetallic compounds Al_3Zr and AlB_2 are not observed which indicates the completeness of reaction, further, it is also evident that no reaction has taken place at the interface of the AA5052 and ZrB_2. XRD pattern of extracted ZrB_2 is shown in Fig. 2b, further confirmed the absence of any other intermetallic compound in composites.

3.2 Optical microscopy and grain refinement

Figure 3 shows the optical micrographs of as cast base alloy and in-situ AA5052/9 vol. ZrB_2 composite. It is observed from the micrographs that in-situ formed ZrB_2 particles appear in inter granular regions with agglomeration or clustering.

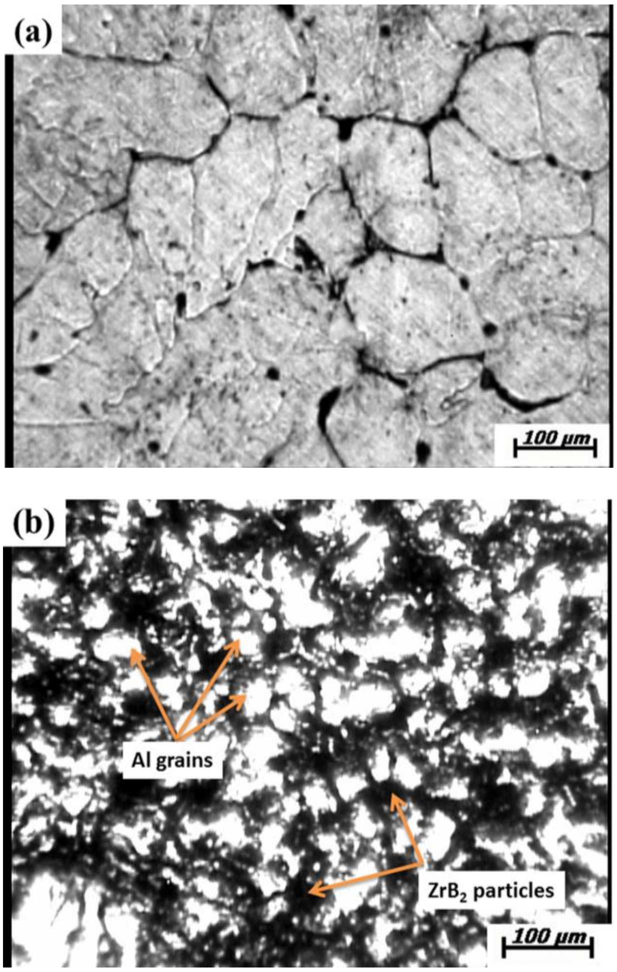

Fig. 3. Optical micrographs of (a) As cast AA5052 alloy (b) 9 vol.% ZrB_2 composite.

Formation of clustered particles depends on synthesis temperature, holding time, reaction rate and cooling rate [27]. Convection current in the melt, movement of solidification front against particles and buoyant motion of particles also affects the distribution of ZrB_2 particles in the melt [28]. Whether the distribution of particles would be intra or inter granular depends on the velocity of solidification front. The particles are pushed by the solidification front to inter granular region if the velocity of solidification front is below a critical velocity and vice versa [29].

Grain refining tendency of ZrB_2 particles is also observed from the microstructure. Grain size of aluminum-rich matrix reduced from about 115 μm to 67 μm with 9 vol.% ZrB_2 composite. The reduction in grain size may be attributed to the restricted growth of Al-rich grains due to the presence of ZrB_2particles during solidification process. ZrB_2 particles act as a nucleus on which aluminum grains solidify [26]. Moreover, increase in ZrB_2 particles with composition creates more nucleation sites due to the under cooling zone in front of ZrB_2 particles. Thus, increased number of ZrB_2 particles provides enhanced resistance to the grain growth of Al-rich phase and results in refined microstructure [29].

3.3 SEM Examination and EDS Analysis

Figures 4a, b and c show the SEM micrographs of the composites with different volume fraction of ZrB_2 particles. Clusters of in-situ formed ZrB_2 particles were observed in the matrix but these clusters were uniformly distributed all over the matrix.

Figures 5a and b show hexagonal and rectangular morphology of ZrB_2 particles at higher magnification. The difference in shapes may be attributed to the fracture of column-like particles generated in the melt [30,31]. Most of the ZrB_2 particles were of nanometer size and few of micron size ranging from 25 nm-2 μm. Magnesium accelerates nucleation rate of ZrB_2 particles and promotes the formation of fine ZrB_2 particles [32]. EDS spectrum of in-situ formed ZrB_2 particle is shown in Fig. 5c, with peaks of Al, Zr and B elements only which further confirms the presence of ZrB_2 compound in the aluminum matrix.

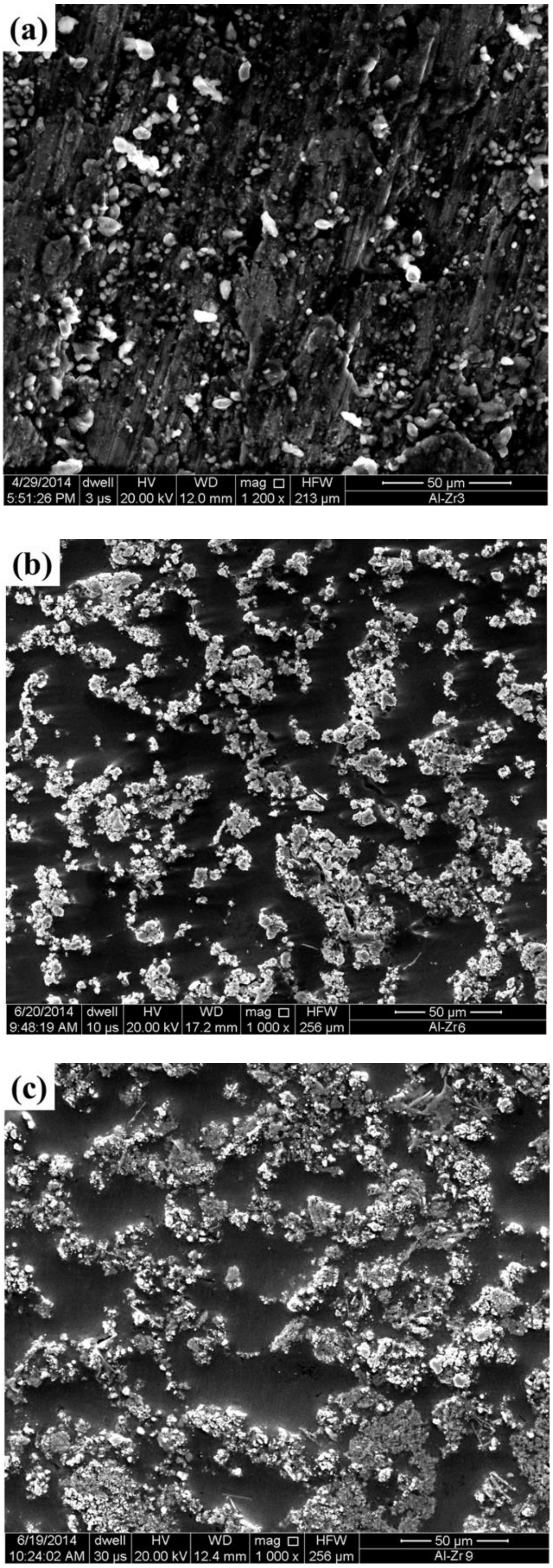

Fig. 4. SEM micrographs of (a) AA5052-3 vol.% ZrB_2, (b)AA5052-6 vol.% ZrB_2,(c) AA5052-9 vol.% ZrB_2.

3.4 TEM Analysis

TEM study was carried out to reveal the crystal structure, interfacial characteristics and dislocations in the matrix around ZrB_2 particles.

Figure 6a shows the insitu formed ZrB_2 particle and matrix.It is also evident that interface between the matrix and particle is clear and well bonded. Interface is also free of porosity and reaction product. Clear interface is essential for improving the load bearing capacity of the composite. Presence of clear interface can be attributed to thermodynamic stability of ZrB_2 particle and formation of ZrB_2 particles within melt which reduce the probality of oxidation of particles, hence, imroving the interfacial bonding between matrix and particles.

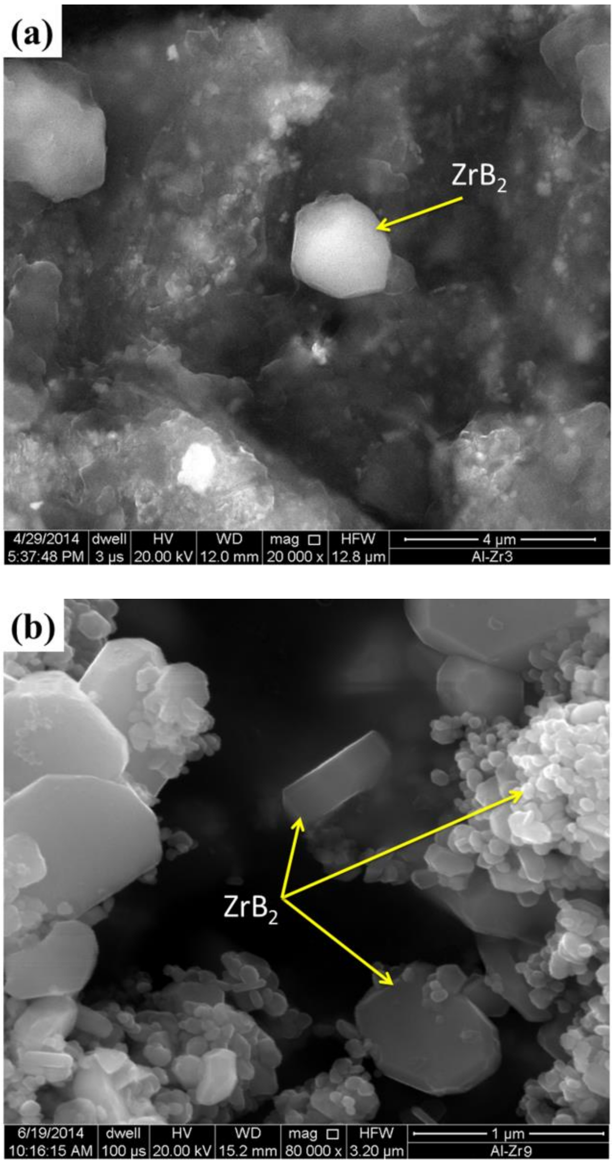

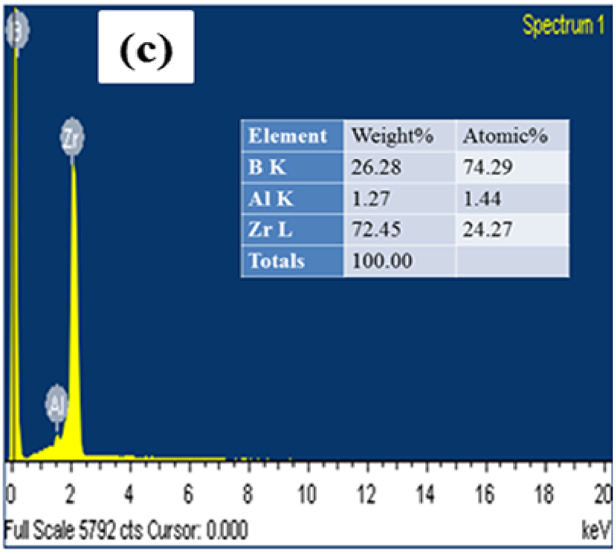

Fig. 5. (a) and (b) Morphology of ZrB_2particle at higher magnification (c) EDS spectrum of ZrB_2.

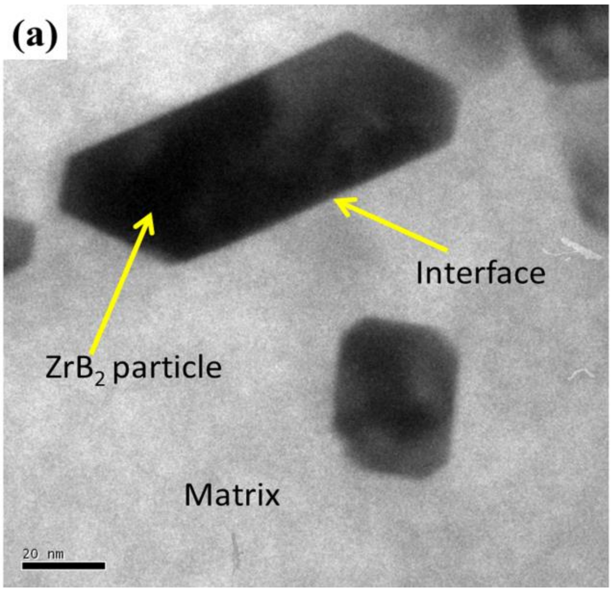

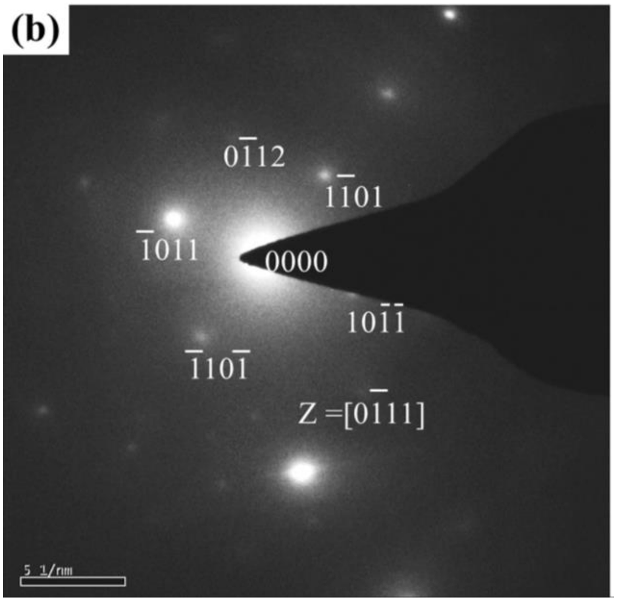

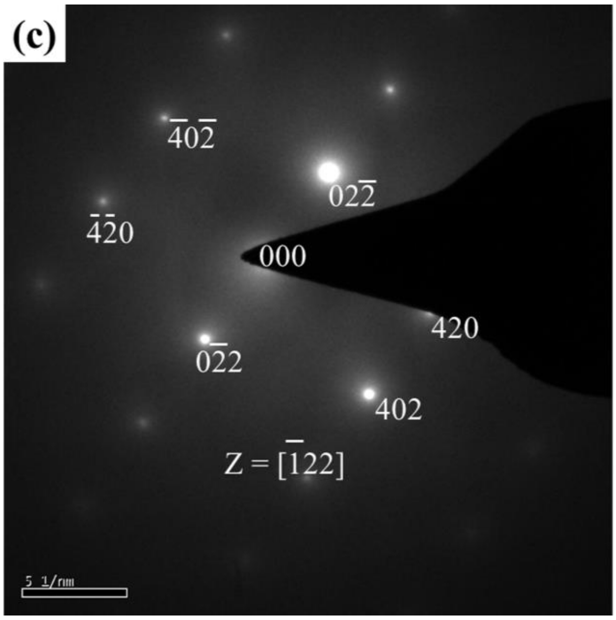

Fig. 6. TEM micrographs of (a) rectangular morphology (b) SAD pattern of ZrB_2 and (c) SAD pattern of matrix.

Figures 6b and c show the selected area diffraction (SAD) pattern of the ZrB_2 particle and matrix. Their analysis shows that ZrB_2 has hexagonal close-packed structure (HCP)whereas matrix is face centered cubic (FCC). Figure 7 clearly reveals the presence of dislocations in the matrix due to formation fine ZrB_2 particles.

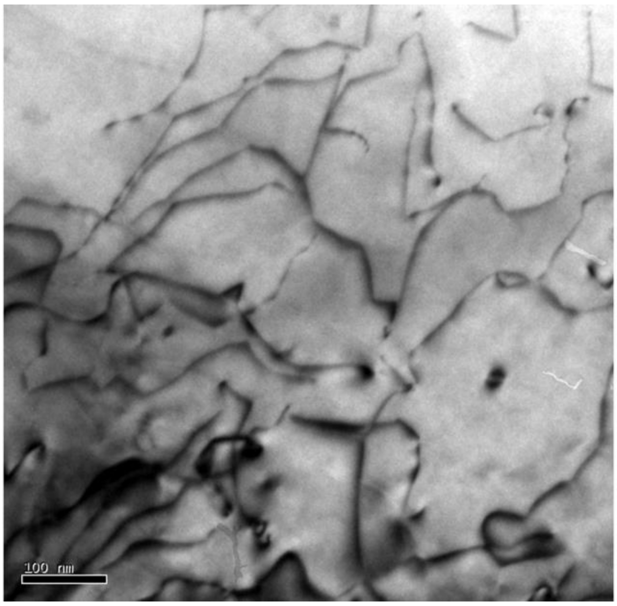

Fig. 7. TEM micrograph showing dislocations present in the matrix.

3.5 Hardness

Figure 8 shows the variation of hardness (BHN) of base alloy and composites with volume percentage of ZrB_2 particles. It is observed that hardness increases with increasing amount of ZrB_2 particles and a maximum of 47 % improvement in hardness has been observed for composite having 9 vol.% ZrB_2 particles as that of the base alloy.

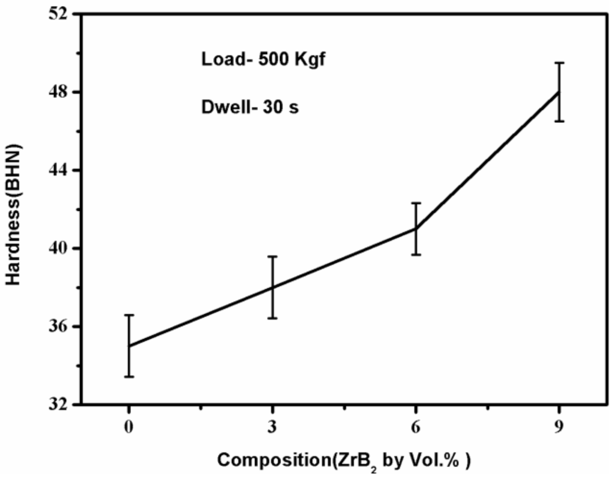

Fig. 8. Variation of hardness with vol.% of ZrB_2.

The reasons for improvement in hardness are high hardness of ZrB_2 particles, high dislocation density around the ZrB_2 particles (Fig. 7) due to difference in coefficient of thermal expansion (CTE) between aluminum matrix and ZrB_2particles [26,33] and restricted growth of aluminum grains during solidification due the presence of fine ZrB_2 particles.

3.6 WEAR AND FRICTION STUDY

Wear behavior of materials is very complex phenomenon due to many variables such as sliding parameters, materials properties, abrasive effects, and lubricating conditions etc. Sliding wear is related to asperity-to-asperity contact of two counter surfaces, which are in relative motion against each other. Effect of various parameters like, sliding distance, applied load and volume fraction of ZrB_2 particles on wear and friction behavior of composites has been discussed in the following sections.

Effect of sliding distance

Figure 9a represents the variation of cumulative weight loss of base alloy and composites as a function of sliding distance at 30 N load and sliding velocity 2.12 m/s. It is observed that wear loss increases with increasing the sliding distance for all composites and base alloy. However, a decrease in wear loss is observed with increasing volume fraction of ZrB_2 particles. It is also observed from this figure that cumulative wear rate increases after sliding a distance of 2400m and 4800m which may be due to the distortion of surface with sliding distance.

Figure 9b shows the variation of the coefficient of friction (COF) with the sliding distance under dry sliding conditions at 40N normal load and for 2.12 m/s sliding velocity with different vol.% of ZrB_2. Coefficient of friction of composites is higher than base alloy while sliding under identical conditions. The higher coefficients of friction in the case of composites are due to the presence of hard particles at the interface between two contacting surfaces. When the effective load on the individual particle is above its flexural strength, the particles get fractured and entrapped within the softer surface and coefficient of friction fluctuates within a value of ±0.025.

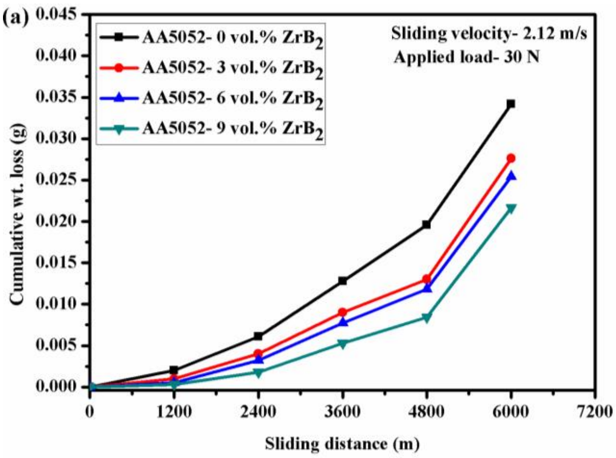

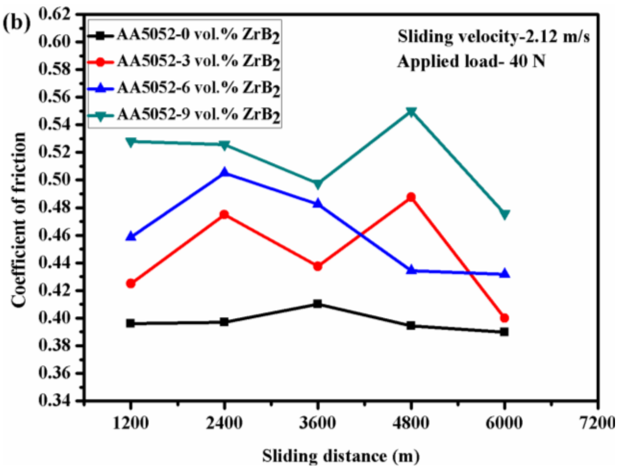

Fig. 9. Variation of (a) cumulative wt. loss and (b) COF with sliding distance.

Figure 10(a) and (b) reveal the morphology of the worn surfaces of 6 vol.% ZrB_2 composite at 2.12 m/s sliding velocity and 30 N load after sliding 1200 m and 6000 m distance. Fig. 10a reveal the shallow ploughing marks and grooves, no delamination is observed at 1200 m whereas in Fig. 10b deep ploughing and grooves with high degree of delamination are visible after sliding distance of 6000 m.

Effect of applied load

It is evident from Fig. 11a, that wear rate increases with increase in applied load for both unreinforced alloy as well as composites. At low loads wear rate increases linearly but after 30 N load transitions in wear nature takes place from mild to severe and a sudden increase in wear rate is observed.

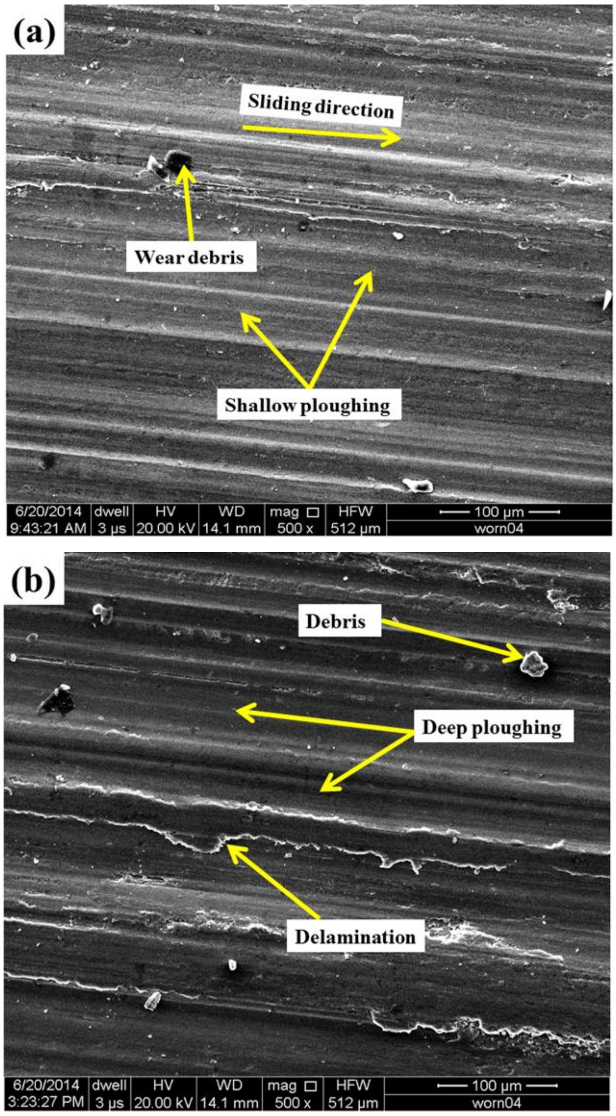

Fig. 10. Wear surface morphology of 6 vol.% ZrB_2 composite at 30 N load and 2.12 m/s sliding velocity after sliding distance of (a) 1200 m (b) 6000m.

The reason for increased wear rate may be due increases in contact area between the two surfaces with increase in load, which leads to generation of high amount of frictional heat between the surfaces. High fictional heating results in softening of the pin surface and increased wear rate due to more penetration of hard asperities into soft pin surface. The increase in the applied load may also lead to increase in micro cracking tendency of the subsurface as well as deformation and fracture of asperities. These asperities are either removed from the surface or deformed in the sub-surface. In the presence of hard ZrB_2 particles a mechanically mixed layer (MML) of soft aluminum base matrix and hard particles of ZrB_2 is formed (Figs. 12a and b). At low loads this MML restricts the transfer of material from the surface and the wear rate is less, or it is in mild wear regime and oxidative wear dominates. But, after a transition load of 30N cracking of this MML takes place and hard ZrB_2 particles come out (Fig. 12c) and act as third body abrasion and wear mechanism changes from mild to severe giving rise to oxidative-metallic wear as observed in Fig 11a, and the wear rate increases.

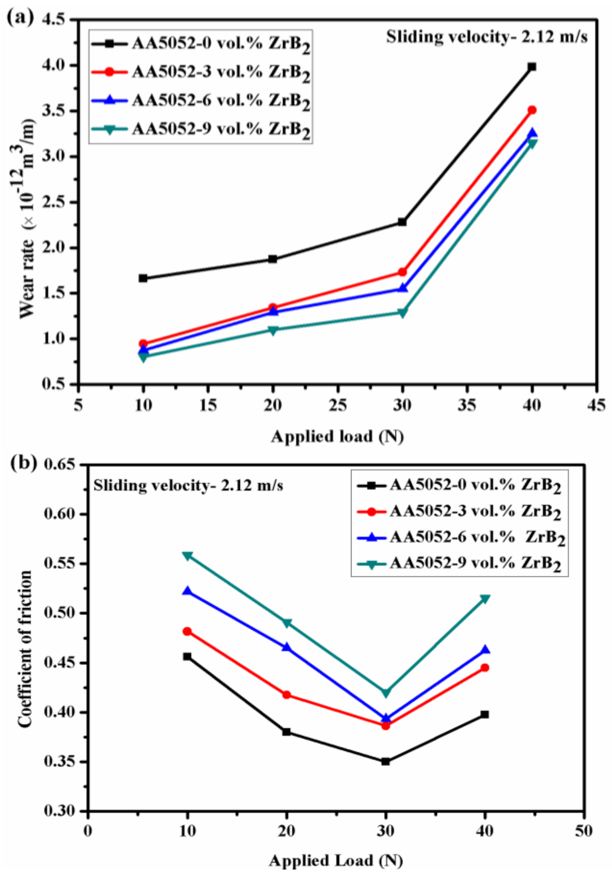

Fig. 11. (a) Variation of wear rate with applied load and (b) Variation of COF with applied load.

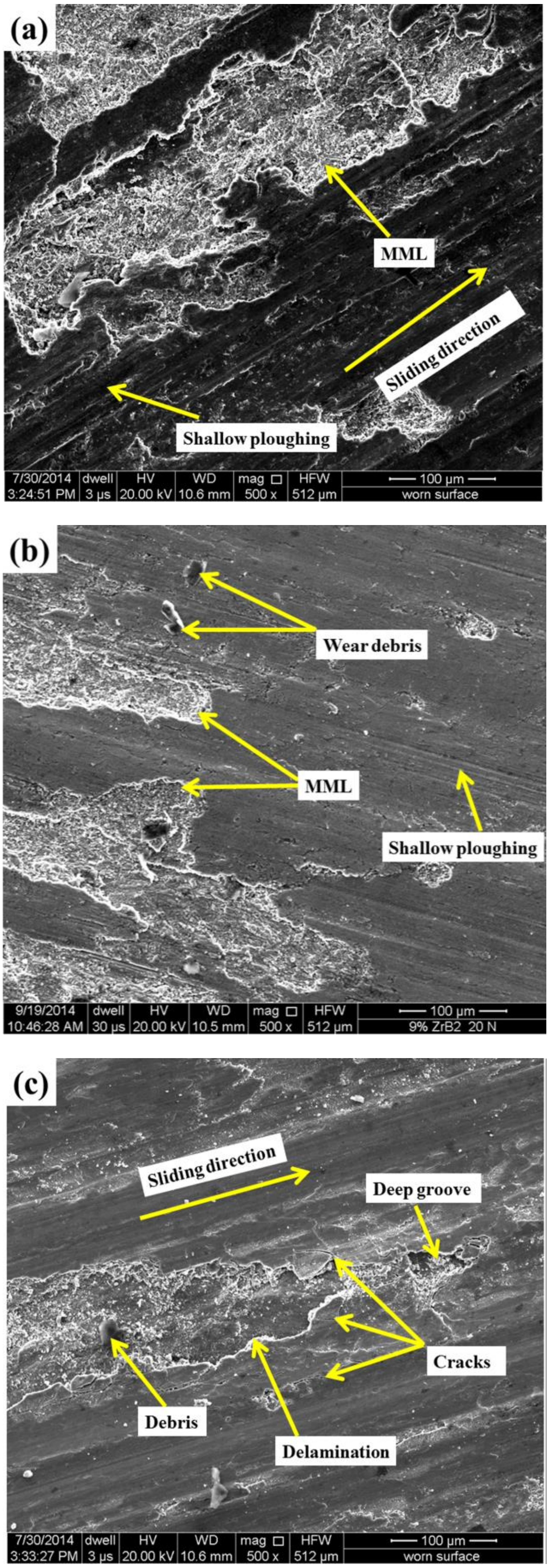

Fig. 12. SEM micrographs of wear tracks at different loads for composite with 9 vol.% ZrB_2 particles at 2.12 m/s sliding velocity (a) 10 N, (b) 20 N and (c) 40 N.

At low loads wear surface morphology exhibits relatively smooth areas with shallow grooves, (Fig. 12a and b) but as the load increases MML is broken, and wear surface exhibits deep grooves, severely damaged areas, delamination and large number of cracks (Fig. 12c) which leads to the increased wear rate. Initially, coefficient of friction decreases with load up to 30 N but at higher load i.e. beyond 30N formation for larger small hard particles of ZrB_2 in MML contributes to friction and it starts increasing with load (Fig. 11b).

Effect of volume fraction of ZrB_2 particles

Wear rate of the composites decreases with increase in volume fraction of ZrB_2 particles at a constant sliding velocity of 2.12 m/s and at different applied loads of 10 N, 20 N, 30 N and 40 N as evident from the Fig. 13a. This may be due to refinement of Al-grains and good interfacial bonding between the matrix and ZrB_2 particles which enhance the load bearing capacity of composites [34]. It is reported that fine grain structure consists of more grain boundary per unit area of Al matrix, which enables higher load bearing capacity and wear resistance as compared to the coarse grain structure [35]. Also in addition, ZrB_2 particles reduce the extent of direct metal-to-metal contact between matrix and counterface, thus, ZrB_2 particles act as a load bearing phase and protects the matrix during sliding process.

An increase in the volume fraction of ZrB_2 particles results in an increase in dislocation density around the ZrB_2 particles during solidification hence, strength and hardness of composites improve which contributes to lower the wear rate [36]. Further, increase in percentage of ZrB_2 in MML also restricts the removal of material from the surface due to increased hardness of composite and wear rate decreases (Figs. 14a and b) which is in agreement with Archard's wear law [37].

Hence, wear rate of composites reduces with the content of ZrB_2. This can be attributed to the increase in hardness due to the refinement of grain size, reinforcement of hard ceramic ZrB_2 particles, good interfacial bonding and presence of MML.

Figure 13b shows the variation of average coefficient of friction with vol.% of ZrB_2 particles at 40 N applied load and sliding velocity 2.12 m/s. It is observed that coefficient of friction increases with increasing the vol.% ZrB_2 particles. With increase in the amount of ZrB_2 particles in the MML total coefficient of friction increase as a result of increased presence of large abrasive particles where as other factors contributing to friction remain more or less same, and a continuous increase in coefficient of friction is observed.

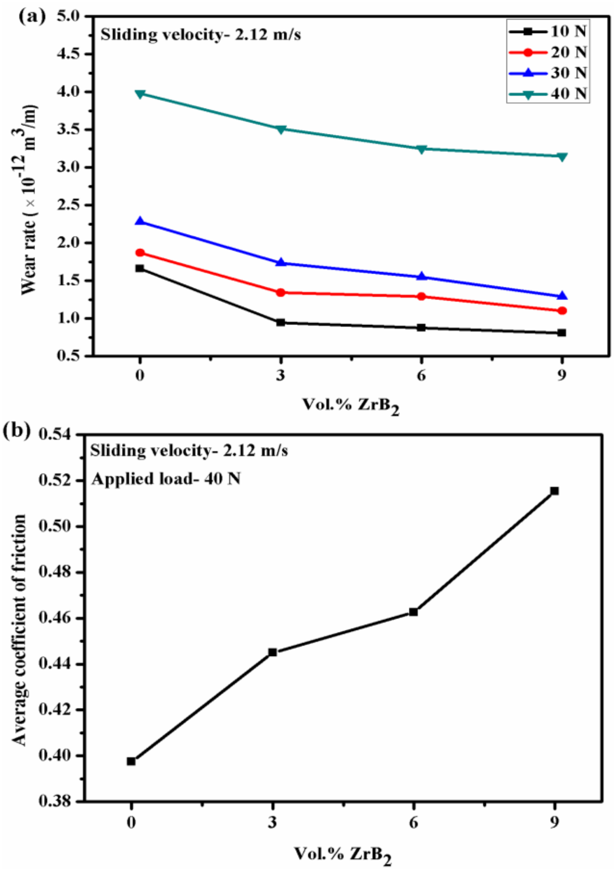

Fig. 13. Variation of (a) wear rate with vol.% ZrB_2 (b) COF with vol.% ZrB_2.

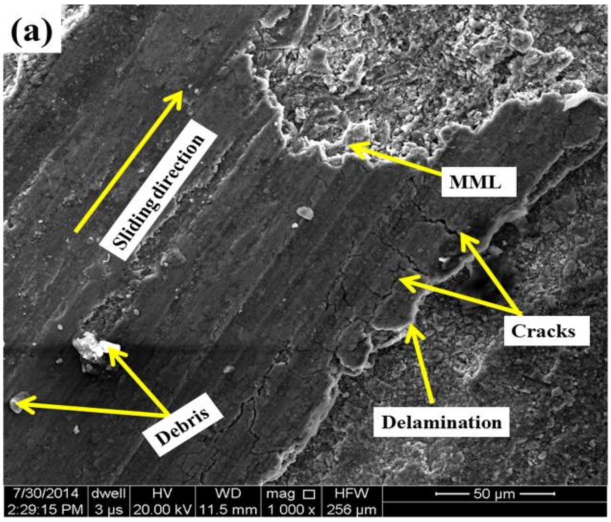

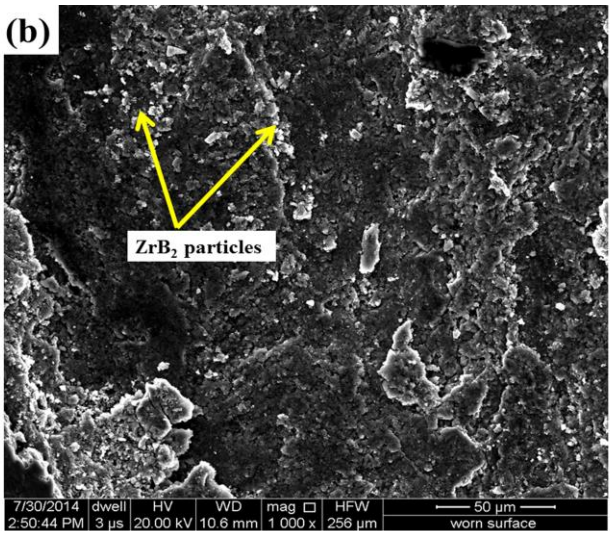

Fig. 14. SEM micrographs of wear tracks of composites with different % ZrB_2 particles at 30 N load and 2.12 m/s sliding velocity showing larger number of particles in MML (a) 3 vol.% and (b) 9 vol.%.

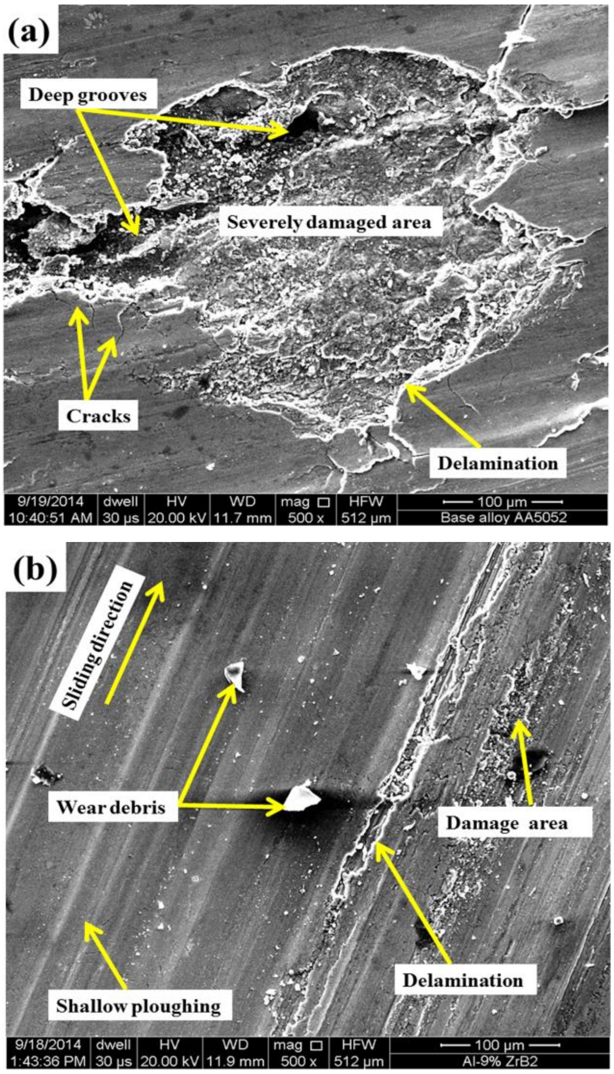

Fig. 15. Wear surface morphology of (a) AA5052 alloy (b) 9 vol.% ZrB_2 composite at 20 N load and 2.12 m/s sliding velocity.

Figure 15(a) and (b) reveal morphology of the worn surfaces of AA5052 matrix alloy and AA5052/ 9 vol.% ZrB_2 composite at 20 N load and 2.12 m/s sliding velocity. Wear surface of matrix alloy (Fig. 15 (a)) exhibits deep grooves, large number of cracks, delamination and severely damaged areas which may be due the generation of high frictional heating between the surfaces whereas shallow grooves, less delamination and damaged area are seen in Fig.15 (b). The wear debris is loose in nature and not adhering to the surface due to hard ZrB_2 particles. It is clear from the wear surfaces that wear rate decreases when the content of ZrB_2 particle increases.

4. CONCLUSION

It can be concluded from the present study that:

1. AA5052/ZrB_2 in-situ composites can be successfully prepared by in-situ reaction between inorganic salts K_2ZrF_6, KBF_4 and AA5052 aluminum alloy.
2. In-situ formation of ZrB_2 particles refines matrix, creates dislocation and improves the hardness of composite which leads to the reduced wear loss.
3. Clear interface between matrix and ZrB_2 particle exhibits good bonding resulting in the enhanced load bearing capacity of composites.
4. Cumulative wear increases continuously but after certain intervals of sliding distance, wear rate increases.
5. Wear rate continuously increases with load but after 30 N of load wear changes from mild to severe, whereas, with increase in the amount of ZrB_2 particles wear rate continuously decreases.
6. Coefficient of friction fluctuates with a value of ±0.025 with sliding distance, however, with load it decreases up to 30 N but beyond this value it starts increasing.
7. Coefficient of friction increases continuously with increasing amount of ZrB_2 particles.

Acknowledgements

Corresponding author gratefully acknowledges All India Council for Technical Education, New Delhi, India for providing financial assistance under its QIP scheme. He is also thankful to Director, BIET Jhansi, for providing leave to carry out this research.

REFERENCES

[1] R. Asthana, 'Reinforced cast metals Part II Evolution of the interface', *J. Mater. Sci.*, vol. 33, no. 8, pp. 1959–1980, 1998.

[2] C.A. Leon and R.A.L. Drew, 'Preparation of Nickle-coated powders as precursors to reinforce MMCs', *J. Mater. Sci.*, vol. 35, no. 19, pp. 4763–4768, 2000.

[3] K.S. Foo, W.M. Banks, A.J. Craven and A. Hendry, 'Interface characterization of an SiC particulate/6061 aluminum alloy composite', *Composites*, vol. 25, no. 7, pp. 677–683, 1994.

[4] R. Shubin, H. Xinbo, Q. Xuanhui and L. Yan, 'Effect of controlled interfacial reaction on the microstructure and properties of the SiCp /Al composites prepared by pressureless infiltration', *J. Alloys Compd.*, vol. 455, no. 1, pp. 424-431, 2008.

[5] D.J. Lioyd, 'Particle reinforced aluminum and magnesium matrix composites', *Int. Mater. Rev.*, vol. 39, pp. 1-23, 1994.

[6] J. Eliasson and R. Sandstorm, 'Applications of aluminum matrix composites', *Key Eng. Mater.*, vol. 104, pp. 3-36, 1995.

[7] S.V. Prasad and R. Asthana, 'Aluminum metal-matrix composites for automotive applications: Tribological considerations', *Tribol. Lett.*, vol. 17, no. 3, pp. 445-453, 2004.

[8] ZY. Liu, QZ. Wang, BL. Xiao, ZY. Ma and Y. Liu, 'Experimental and modelling investigation on SiCp distribution in powder metallurgy processed SiCp/2024 Al composites', *Mater. Sci. Eng., A*, vol. 527, no. 21, pp. 5582-5591, 2010.

[9] S. Srivastava and S. Mohan, 'Study of wear and friction of Al-Fe metal matrix composites produced by liquid metallurgical method', *Tribology in Industry*, vol. 33, no. 3, pp. 128-137, 2011.

[10] Y. Iwai, T.Honda, T. Miyajima, Y. Iwasaki, M.K. Surappa and J.F. Xu, 'Dry sliding wear behavior of Al_2O_3fiber reinforced aluminum composites', *Compos. Sci. Technol.*, vol. 60, no. 9, pp. 1781-1789, 2000.

[11] AM. Hassan, A. Alrashdan, MT. Hayajneh and AT. Mayyas, 'Wear behavior of Al–Mg–Cu–based composites containing SiC particles', *Tribol. Int.*, vol. 42, no. 8, pp. 1230–1238, 2009.

[12] M. Zhao, G. Wu, L. Jiang and Z. Dou, 'Friction and wear properties of TiB_{2P}/Al composite', *Compos Part A - Appl S.*, vol. 37, no. 11, pp. 1916–1921, 2006.

[13] C.S. Ramesh, R. Keshavamurthy, B.H. Channabasappa and S. Pramod, 'Friction and wear behavior of Ni-P coated Si_3N_4 reinforced Al6061 composites', *Tribol. Int.*, vol. 43, no. 3, pp. 623-634, 2010.

[14] Z. Yutao, Z. Songli, C. Gang, C. Xiaonong and D. Qixun, '(ZrB_2 +Al_2O_3 +Al_3Zr)p/Al–4Cu composite synthesized by magneto-chemical melt reaction', *Mater. Sci. Eng., A*, vol. 487, no. 1, pp. 1–6, 2008.

[15] Z. Heguo, J. Cuicui, S. Jinzhu, Z. Jun, L. Jianliang and X. Zonghan, 'High temperature dry sliding friction and wear behavior of aluminum matrix composites (Al_3Zr+α-Al_2O_3)/Al', *Tribol. Int.*, vol. 48, pp. 78–86, 2012.

[16] XH. Zhang, L. Xu, SY. Du, JC. Han, P. Hu and WB. Han, 'Fabrication and mechanical properties of ZrB_2-SiC_w ceramic matrix composite', *Mater. Lett.*, vol. 62, pp. 1058–1060, 2008.

[17] Z. Xinghong, L. Xiaoguang, L. Jinping, H. Jiecai, H. Wenbo and H. Changqing, 'Structure and bonding features of ZrB_2 (0001) surface', *Comput. Mater. Sci.,* vol. 46, no. 1, pp. 1-6, 2009.

[18] Z. Songli, Z. Yutao, C. Gang and C. Xiaonong, 'Microstructures and dry sliding wear properties of in situ (Al_3Zr + ZrB_2)/Al composites', *J. Mater. Process. Technol.*, vol. 184, pp. 201–208, 2007.

[19] Z. Songli, Z. Yutao, C. Gang, C. Xiao-Nong and H. Xiao-Yang, 'Fabrication and dry sliding wear behavior of in situ Al–K_2ZrF_6–KBF_4 composites reinforced by Al_3Zr and ZrB_2 particles', *J. Alloys Compd.*, vol. 450, pp. 185–192, 2008.

[20] G. Naveen Kumar, R. Narayanasamy, S. Natarajan, S.P. Kumaresh Babu, K. Sivaprasad and S. Sivasankaran, 'Dry sliding wear behavior of AA 6351-ZrB_2 in situ composite at room temperature', *Mater Design*, vol. 31, pp. 1526–1532, 2010.

[21] I. Dinaharan and N. Murugan, 'Dry sliding wear behavior of AA6061/ZrB_2 in-situ composite', *Trans. Nonferrous Met. Soc. China*, vol. 22, pp. 810-818, 2012.

[22] C. Dengbin, Z. Yutao, Z. Haiyan and C. Gang, 'Microstructures and dry sliding wear properties of ZrB_2/A356 composites synthesized by magneto-chemistry in situ reaction', *Journal of Wuhan University of Technology-Mater. Sci.,* vol. 28, no. 2, pp. 384-388, 2013.

[23] R. Gurler, 'Sliding wear behavior of a silicon carbide particle-reinforced aluminum-magnesium alloy', *J. Mater. Sci. Lett.*, vol. 18, pp. 553-554, 1999.

[24] H. Sekine and R. Chent, 'A combined microstructure strengthening analysis of SiC_p /Al metal matrix composites', *Composites*, vol. 26, no. 3, pp. 183-188, 1995.

[25] F. Rana and D.M. Stefanescu, 'Friction properties of Al/1.5 Pct Mg/SiC particulate metal matrix composites', *Metall. Trans. A,* vol. 20, no. 8, pp. 1564-1566, 1989.

[26] I. Dinaharan, N. Murugan and S. Parameswaran, 'Influence of in situ formed ZrB_2 particles on microstructure and mechanical properties of AA6061 metal matrix composites', *Mater. Sci. Eng. A.*, vol. 528, pp. 5733–5740, 2011.

[27] SC. Tjong and ZY. Ma, 'Microstructural and mechanical characteristics of in situ metal matrix composites', *Mater. Sci. Eng. R.*, vol. 29, pp. 49-113, 2000.

[28] R. Bauri, D. Yadav, G. Suhas, 'Effect of friction stir processing (FSP) on microstructure and properties of Al-TiC in situ composite', *Mater. Sci. Eng A.*, vol. 528, pp. 4732-4739, 2011.

[29] HM. Rajan, S. Ramabalan, I. Dinaharan and SJ. Vijay, 'Synthesis and characterization of in situ formed titanium diboride particulate reinforced AA7075 aluminum alloy cast composite', *Mater Design*, vol. 44, pp. 438- 445, 2013.

[30] K. Tian, Y. Zhao, L. Jiao, S. Zhang, Z. Zhang and X. Wu, 'Effects of in situ generated ZrB_2 nano-particles on microstructure and tensile properties of 2024Al matrix composites', *J. Alloys Compd.*, vol. 594, pp. 1–6, 2014.

[31] W. Jiangjing, Z. Yutao, Z. Songli, C. Gang and Z. Zhenya, 'Effects of in-situ ZrB_2 particle on grain refinement of ZrB_2/AZ91D magnesium matrix composite', *China Foundry*, vol. 9, pp. 28–33, 2012.

[32] AK. Lohar, BN. Mondal and SC. Panigrahi, 'Effect of Mg on the microstructure and mechanical properties of Al0.3Sc0.15Zr-TiB_2 composite', *J. Mater. Eng. Perform.*, vol. 20, pp. 1575–1582, 2011.

[33] D. Mandal, BK. Dutta and SC. Panigrahi, 'Effect of wt% reinforcement on microstructure and mechanical properties of Al-2Mg base short steel fibre composites', *Mater. Process. Tech.*, vol. 198, pp. 195-201, 2008.

[34] CS. Ramesh and A. Ahamed, 'Friction and wear behaviour of cast Al 6063 based in situ metal matrix composites', *Wear*, vol. 271, pp. 1928–1939, 2011.

[35] AKP. Rao, K. Das, BS. Murty and M. Chakraborty, 'Effect of grain refinement on wear properties of Al and Al–7Si alloy', *Wear*, vol. 257, pp. 148–153, 2004.

[36] M. Gupta and TS. Srivatsan, 'Interrelationship between matrix microhardness and ultimate tensile strength of discontinuous particulate-reinforced aluminium alloy composites', *Mater. Lett.*, vol. 51, pp. 255–261, 2001.

[37] J.F. Archard, 'Contact and rubbing of flat Surfaces', *J. Appl. Phys.*, vol. 24, pp. 981–988, 1953.